

## Influence of soil properties and geometrical characteristics of sediment-filled valleys on earthquake response spectra

LE PENSE S.<sup>1</sup>, GATMIRI B.<sup>2,3,1</sup>, MAGHOUL P.<sup>1</sup>

<sup>1</sup>Université Paris-Est, Laboratoire Navier (ENPC/IFSTTAR/CNRS), École des Ponts ParisTech,  
6 & 8 Avenue Blaise Pascal, 77455 Marne la Vallée, France

<sup>2</sup>Department of Civil Engineering, University of Tehran, P.O. Box 11365-4563, Tehran, Iran

<sup>3</sup>ANDRA, Direction Scientifique, Parc de la Croix Blanche, 1-7 rue Jean Monnet, 92298 Chatenay-Malabry, France  
email: solenn.le-pense@cermes.enpc.fr, behrouz.gatmiri@andra.fr, pooneh.maghou.1@ulaval.ca

**ABSTRACT:** It is well-known that the response of a site to seismic excitation depends on both its local topography and its soil properties. Although the recent building codes (i.e. Eurocode8) incorporate these site effects, they only take into account unidimensional ones and ignore complex cases due to two-dimensional irregular configurations. Recent work has been mainly focusing either on the development of numerical methods allowing always more precise results or on the elaboration of simplified approaches usable for engineering purposes. The aim of this work is to propose a simple criterion, combining soil properties and geometrical characteristics of valleys to estimate the amplification of earthquake response spectra in sediment-filled valleys. We will first study the response of unidimensional soil layers to obtain a criterion that can be extended to bidimensional configurations. The seismic input is a synthetic SV Ricker wave with vertical incidence. Horizontal displacements at surface points are computed by using the HYBRID code which combines finite elements in the near field and boundary elements in the far field (FEM/BEM).

**KEY WORDS:** Seismic site effect; Seismic amplification; Building codes; Seismic response spectrum; Hybrid numerical method; Sedimentary valley; 2D configurations.

### 1 INTRODUCTION

Earthquakes are caused by sudden slips on geological faults. Seismic waves are then generated and propagate through the lithosphere up to the earth surface. The induced seismic movement depends on the earthquake magnitude (the energy produced by the source), but also on the path followed within the lithosphere (regional hazard) and on local conditions (local hazard).

The modification of the seismic movement due to local topographical and geotechnical conditions is called *site effect*. This amplification, or attenuation is obtained by comparing the response of a site with the one of a reference site, i.e. a site located on flat rock. These site effects are mainly observed at the top of hills or in alluvial valleys, where buildings suffer greater damage than might have been expected from their distance to the epicentre.

The most famous example of this phenomenon is the 1985 Michoacan earthquake, during which the city of Mexico, located 400 km from the epicentre, was greatly damaged. The maximum acceleration recorded in the valley had been five times higher than at a nearby site located on rock.

Even though one-dimensional (1D) site effects have already been incorporated in current building codes, there is still progress to be made in taking into consideration complex site effects due to two-dimensional (2D) irregular configurations.

Much work has been done since the 1980s to improve the understanding of the physical phenomena involved in site effects and their prediction. Analytical solutions have been developed for simple configurations [1], [2], [3], [4], [5]. Simultaneously,

experimental methods have been developed to make the most of in-situ measurements [6].

More recently, the development of numerical methods has made it possible to study site effects for more complex configurations. Gatmiri and his coworkers have developed a program combining finite elements in the near field and boundary elements in the far field (FEM/BEM) called HYBRID [7], [8].

Several researchers have been working on the development of simple criteria allowing the prediction of the amplification due to site effects.

Gatmiri and Arson (2008) [9] proposed a quantitative method to predict horizontal surface displacements. They used independent factors representing the contribution of the following geometrical parameters controlling site effects : location of the site in the valley, filling ratio, depth, slope and shape.

Gatmiri *et al.* (2009) [10] showed that in the central zone of a sedimentary valley, geological effects prevail upon topographical effects, whereas from the mid-slope point up to the edge of the valley topographical effects prevail in the site response. They also introduced a criterion for empty valleys,  $S/A$  (Surface/Angle), with which the amplification at the top corner increases (figure 1).

Based on these previous studies, the aim of this work is to propose a simple criterion combining soil properties and geometrical characteristics, for estimating the amplification of earthquake response spectra in sedimentary valleys.



Figure 1. Definition of parameter  $S/A$

We computed horizontal displacements at the surface of sedimentary valleys by using the HYBRID code. A parametric study is conducted to evaluate the effects of various parameters on the amplification of the response spectrum. Calculations are made for several site locations at the surface of valleys (more than 20 points per valley).

The seismic solicitation is a vertically incident SV Ricker wave. See figure 2 and equations 1 and 2 for its definition.

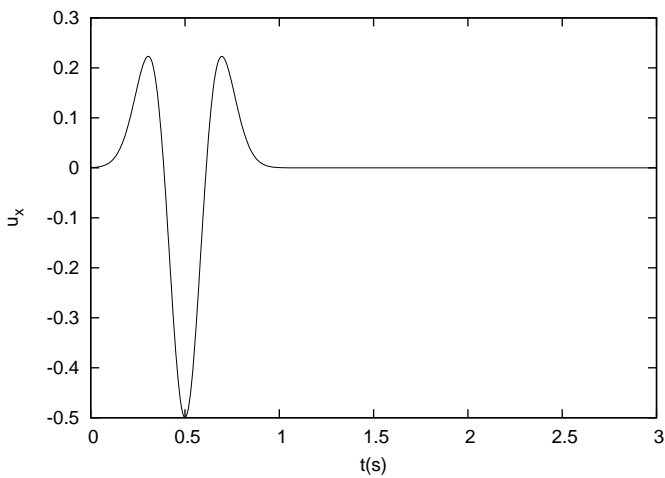


Figure 2. Incident Ricker signal

$$u(t) = A_0(a^2 - 0.5) \exp(-a^2) \tag{1}$$

$$a = \frac{(t - t_s)}{t_p}; \quad A_0 = 1; \quad t_s = t_p = 0.5 \text{ s} \tag{2}$$

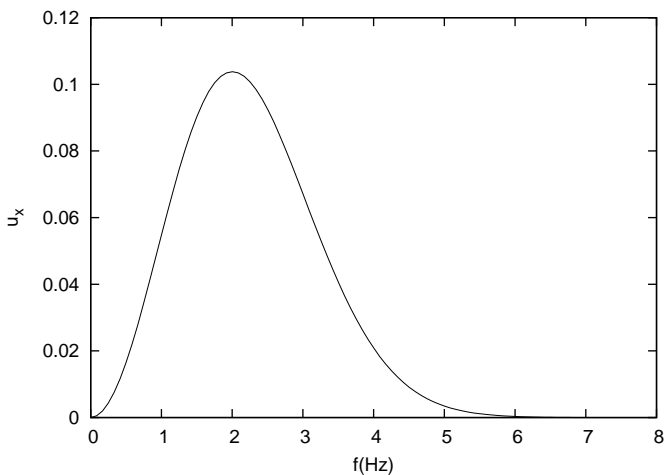


Figure 3. Fourier transform of the reference displacement

In this study, soils are assumed to be dry and linearly elastic. The predominant frequency of the incident signal is fixed and equal to 2 Hz (figure 3).

The reference is taken as the scattering of the Ricker incident wave on a flat bedrock surface.

## 2 METHOD

Several parameters of the seismic movement can be used to characterise site effects, such as the maximum acceleration, velocity or displacement or the duration of the earthquake.

Another very common representation of seismic movement used by engineers is the response spectrum. This is a plot of the maximum response of a family of damped single-degree-of-freedom oscillators to earthquake ground motion. The pseudo-acceleration response spectrum gives an estimate of the maximum acceleration at the base of the building as a function of the natural period of the oscillator  $T_n$ .

For each case, we calculate the earthquake response spectrum with 5% damping and compare it with the reference spectrum (figure 4).

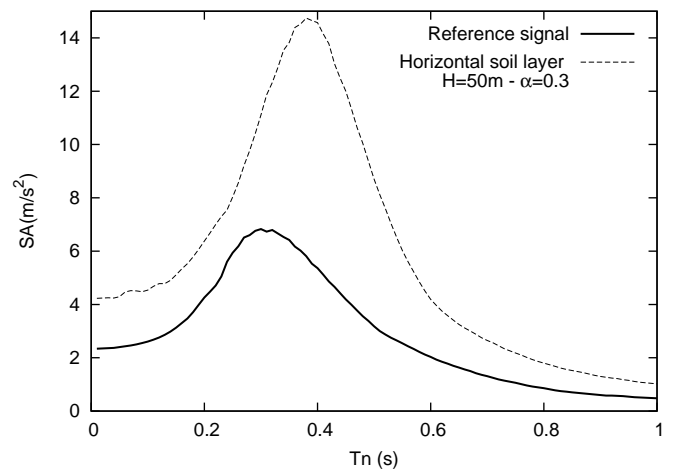


Figure 4. Elastic acceleration response spectra with 5 % damping

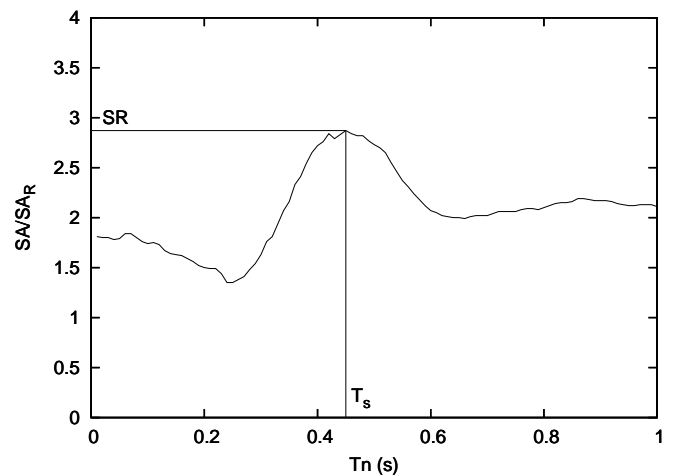


Figure 5. Definition of  $SR$  and  $T_s$

The spectral ratio,  $SR$ , is defined as the maximum ratio between the pseudo-acceleration  $SA$  and the pseudo-acceleration of the reference spectrum  $SA_R$ , for  $T_n$  from 0.1 to 1 second. The site period,  $T_s$ , is defined as the natural period for which this ratio  $SA/SA_R$  reaches its peak (figure 5).

### 3 1D SITE EFFECTS

#### 3.1 Soil properties

The different parameters involved in the site response are the following :

$E$	Young's modulus (MPa)
$K$	Bulk modulus (MPa)
$\nu$	Poisson's ratio
$G$	Shear modulus (MPa)
$\rho$	Density ( $T/m^3$ )
$C$	Wave velocity (m/s)
$\beta$	Impedance contrast between sediments and bedrock
$\rho_s$	Soil density ( $T/m^3$ )
$C_s$	Shear wave velocity in sediments (m/s)
$\rho_r$	Bedrock density ( $T/m^3$ )
$C_r$	Shear wave velocity in bedrock (m/s)

Their different values chosen for sediments and bedrock are given in table 1.

Table 1. Values for bedrock (B) and sediments (S)

	$E$	$K$	$\nu$	$G$	$\rho$	$C$	$\beta$
B	6 720	11 200	0.4	2 400	2.45	990	
S	382	318	0.3	147	1.63	300	<b>0.2</b>
	899	750	0.3	346	1.63	461	<b>0.3</b>
	1 527	1 272	0.3	587	1.63	600	<b>0.4</b>
	2 385	1 988	0.3	917	1.63	750	<b>0.5</b>

The impedance contrast between sediments and bedrock characterises the soil properties (equation 3). The lower the impedance contrast, the softer the sediments are compared to the bedrock.

$$\beta = \frac{\rho_s C_s}{\rho_r C_r} \quad (3)$$

#### 3.2 Analytical solution

In the first place, we consider the simple case of an horizontal soil layer over a semi-infinite elastic space submitted to an harmonic plane S wave (figure 6). We know the analytical formula of the ratio between the displacements at the surface point A and at point B located at the interface between the soil layer and bedrock [11] (See figure 7 and equation 4).

$$\frac{u_A}{u_B} = \frac{1}{\sqrt{\cos^2(k_s \cdot H) + \beta^2 \cdot \sin^2(k_s \cdot H)}} \quad (4)$$

–  $H$  is the soil layer height.

–  $k_s = \frac{2\pi f_c}{C_s}$  is the wavenumber where  $C_s$  is the shear wave velocity in sediments and  $f_c$  is the predominant frequency of the input signal.

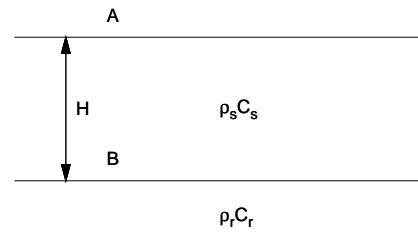


Figure 6. 1D soil layer

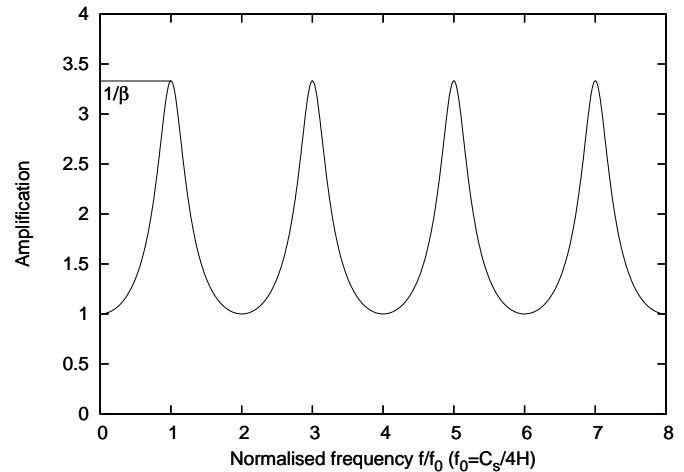


Figure 7. Transfer function for a soil layer

–  $\beta$  is the impedance contrast between sediments and bedrock.

The maximum amplification takes place for specific frequencies (equations 5 and 6).

$$f_n = (2n + 1) \frac{C_s}{4H} \quad (5)$$

$$\left( \frac{u_A}{u_B} \right)_{\max} = \frac{1}{\beta} \quad (6)$$

#### 3.3 Site period $T_s$

We study the seismic response of horizontal soil layers with various heights and impedance contrasts. The height  $H$  varies from 10 m to 100 m and the impedance contrast  $\beta$  varies from 0.2 to 0.5.

We plot some spectra on the same graph to observe the influence of the height of the layer and the impedance contrast on their shapes. We first focus on the site period.

Figure 8 shows the response spectra of layers with a fixed impedance contrast,  $\beta = 0.3$ , and various heights  $H$ . We see that when  $H$  increases,  $T_s$  first increases. If  $H$  keeps increasing, for example for  $H = 100$  m,  $T_s$  goes back to lower periods.

Similarly, figure 9 shows the spectra of layers with a fixed height,  $H = 50$  m, and several values of the impedance contrast  $\beta$ . When  $\beta$  decreases,  $T_s$  increases.

If we suppose that the maximum amplification of the earthquake spectrum takes place for the natural period corresponding

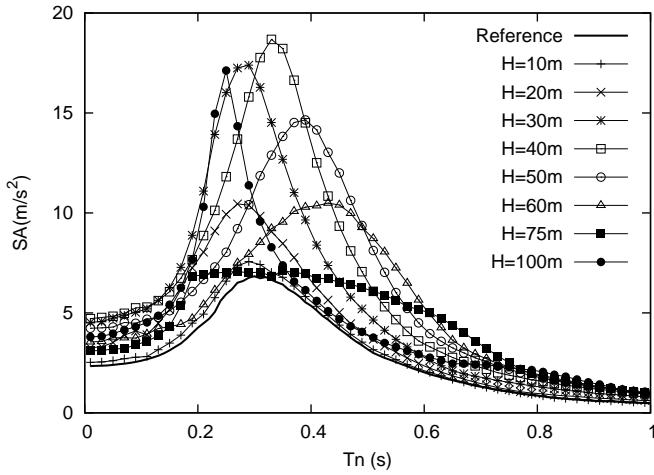


Figure 8. Effect of height on response spectra ( $\beta = 0.3$ )

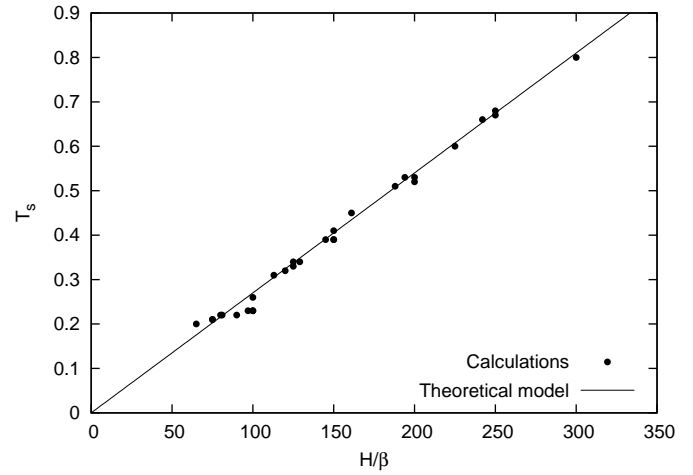


Figure 10. Evolution of  $T_s$  with  $H/\beta$

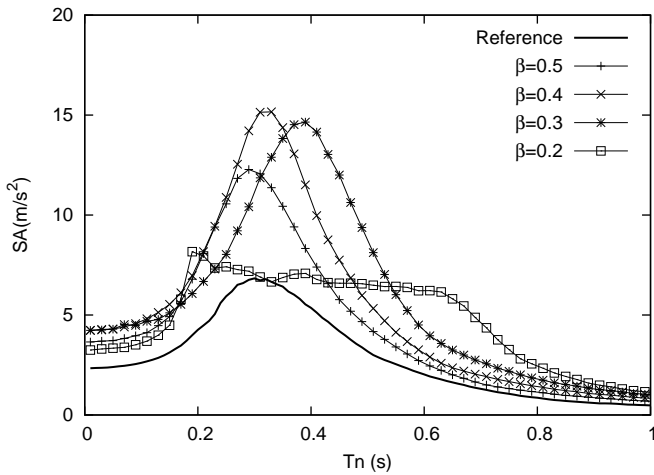


Figure 9. Effect of impedance contrast on response spectra ( $H = 50$  m)

to the fundamental frequency of the soil layer, we obtain an analytical value of  $T_s$  as a function of  $H$  and  $\beta$  (equation 7).

$$T_s = \frac{1}{f_0} = \frac{4H}{C_s} = \frac{4\rho_s}{\rho_r C_r} \frac{H}{\beta} = 0.0027 \frac{H}{\beta} \quad (7)$$

For cases for which the amplification is significant, figure 10 shows the evolution of  $T_s$  with  $H/\beta$  in comparison with the theoretical model  $T_s = 0.0027H/\beta$

For values of  $H/\beta$  from 65 to 300, our set of data is in very good agreement with the theoretical model.

These values of  $H/\beta$  correspond to soil layers with fundamental frequencies between 1.2 and 5.8 Hz, which are the frequencies included into the incident signal (see figure 3).

For higher frequencies (lower values of  $H/\beta$ ) which are absent from the incident signal, the amplification is very weak. It does not allow us to determine an appropriate site period  $T_s$ .

Lower frequencies (higher values of  $H/\beta$ ) correspond to the cases for which the site period  $T_s$  goes back to low period, for high values of  $H$  and low values of  $\beta$ . These frequencies being rare in the incident signal, this phenomenon may be due to a

resonance of the soil layer on a second mode. From now on we will ignore these cases.

As can be seen in figure 10, the correlation between our data and the theory is good enough to validate our approach and extend it to the estimation of the spectral ratio and to bidimensional configurations.

### 3.4 Spectral ratio

To characterise the spectral amplification, we need two criteria : one for estimating the site period and one for estimating the spectral ratio. We first observe how the two parameters,  $H$  and  $\beta$ , influence the amplitude of the response spectra.

Figure 11 shows the response spectra for a wide range of heights for two types of soil : a soft soil ( $\beta = 0.2$ ) and a stiffer soil ( $\beta = 0.4$ ). For a same site period  $T_s$  the amplitude of response spectra is higher for soft soils (lower  $\beta$ ). Since, for a given site period,  $\beta$  and  $H$  are proportional (see equation 7), we will also have higher amplifications for thinner layers (lower  $H$ ). This is confirmed by figure 12 which shows the response spectra for two layer heights ( $H = 30$  m and  $H = 40$  m) for several values of the impedance contrast.

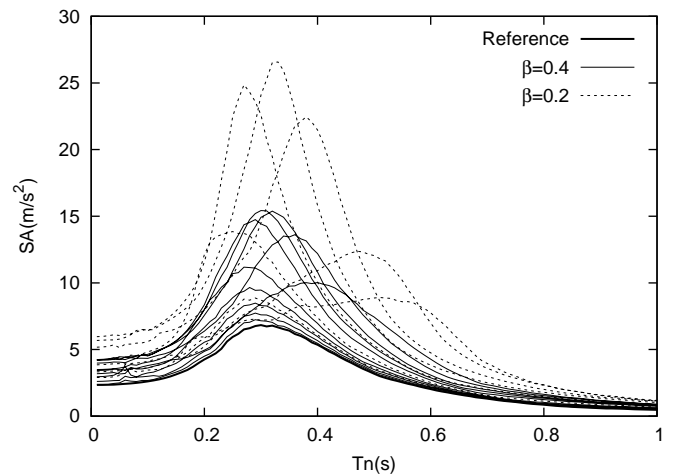


Figure 11. Influence of the impedance contrast on the acceleration response spectra of 1D soil layers

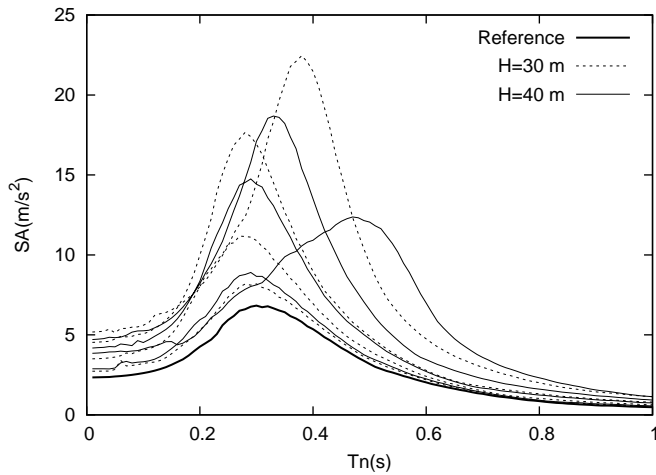


Figure 12. Influence of the layer height on the acceleration response spectra of 1D soil layers

We want to represent on the same graph the spectral ratios for the different soil layers, in order to give a quantitative estimate of the spectral ratio knowing  $H$  and  $\beta$ .

We choose to represent the parameter  $H/\beta$ , which already controls the site period  $T_s$ , on the x-axis, and the parameter  $(SR - 1) \cdot H$  on the y-axis (see figure 13).

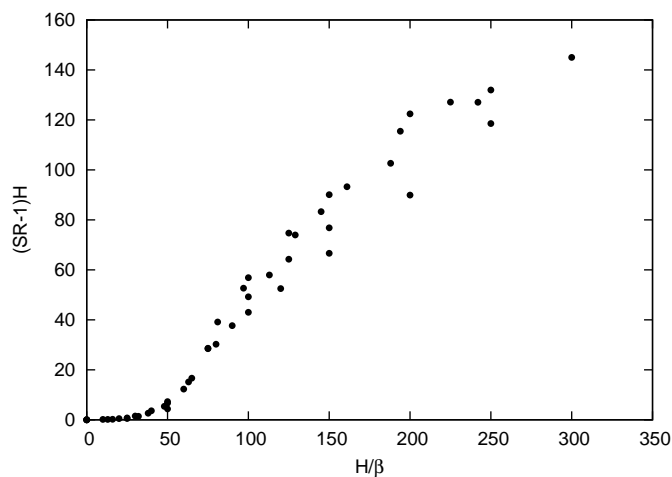


Figure 13. Evolution of  $(SR - 1)H$  with  $H/\beta$

The parameter  $(SR - 1)$  allows us to visualise directly whether or not there is an amplification. Indeed, when there is no amplification  $SR - 1 = 0$ .

This parameter is then multiplied by  $H$  to represent the fact that the spectral ratio decreases when  $H$  increases for a given period.

## 4 2D SITE EFFECTS

### 4.1 Geometrical characteristics

The studied valleys are characterised by their half-width at the surface  $L$ , their half-width at the base  $L_1$ , their depth  $H$  and the sediment layer height  $H_1$ . Let  $A$  be the angle between the slope and the horizontal and  $S_1$  the surface of the section filled with sediments (figure 14).

The half-width  $L$  is equal to 100 m.

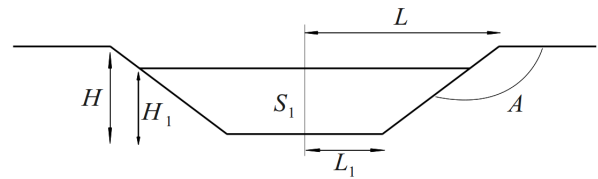


Figure 14. Geometrical parameters

We study trapezoidal valleys corresponding to  $L_1/L = 0.4$ . The calculations are made for different shape ratios  $H/L = 0.2, 0.4, 0.6, 1$  and filling ratios  $H_1/H = 0, 0.25, 0.5, 0.75, 1$ .

### 4.2 Spatial evolution

First, we study the evolution of the spectral ratio with the spatial location of the studied site. The spectral ratio is represented as a function of the non-dimensional variable  $x/L$  for different configurations. On figure 15, we can see the spatial evolution of the spectral ratio, for several filling ratios, for a valley with  $H/L = 0.4$  and  $\beta = 0.2$ .

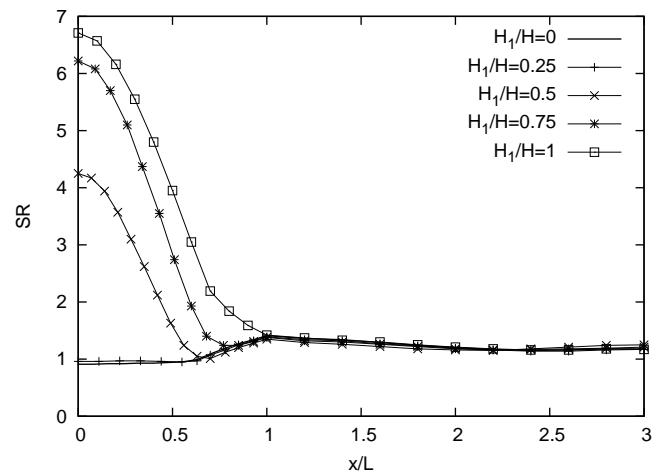


Figure 15. Spatial evolution of spectral ratio for various filling ratios (trapezoidal valley with  $H/L = 0.4$  and  $\beta = 0.2$ )

By increasing the filling ratio, we go from empty valley behaviour with a maximum amplification at the edge of the valley to fully-filled valley behaviour with maximum amplification at the centre of the valley. For a quarter-filled valley the behaviour is the same as that of an empty valley.

For intermediate filling ratios, there is a local maximum at the edge of the valley, a local maximum at the centre of the valley and a minimum at the contact point between sediments and bedrock. There is also a quick decrease of the spectral ratio when moving away from the valley.

From now on, we will focus our study on the amplification at the central point of the valley.

### 4.3 Centre of the valley

#### 4.3.1 Envelope of response spectra

For the different configurations, all the acceleration response spectra calculated at the central point of the valleys are represented on figure 16.

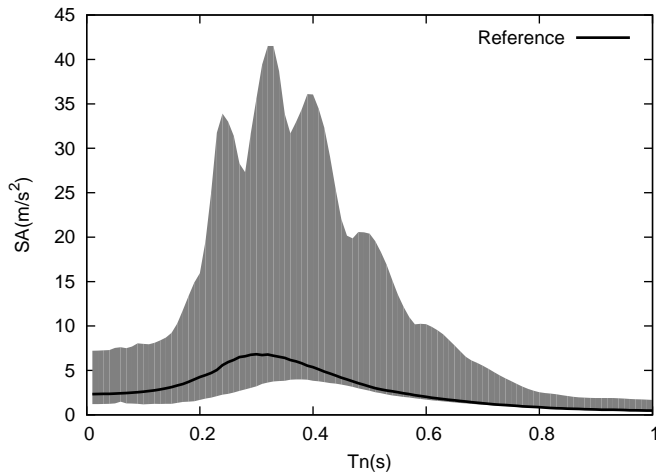


Figure 16. Envelope of response spectra at the centre of the valley for various geometrical characteristics and soil properties.

If there is an attenuation of some spectra for low periods due to topographical effect, it is not significant compared to the amplification of other spectra. Thus, we will not study the attenuation cases afterwards but focus on the amplification cases.

#### 4.3.2 Site period

Following the same method as for 1D soil layers, we want to define a criterion allowing an estimate of the site period for configurations with a significant amplification.

We propose to study the evolution of the site period with the parameter  $S_1/\beta\sqrt{\beta}$  which combines the soil properties ( $\beta$ ) and the geometrical characteristics ( $S_1$ ) (figure 17).

An example of values taken by  $S_1/\beta\sqrt{\beta}$  are given in Table 2.

Table 2. Values taken by  $S_1/\beta\sqrt{\beta}$  for trapezoidal valleys with different shape ratios and filling ratios,  $\beta = 0.3$ .

		filling ratio $L_1/L$			
		0.25	0.5	0.75	1
$H(m)$	20	2,752	6,373	10,863	16,222
	40	5,504	12,746	21,746	32,445
	60	8,256	19,119	32,590	48,667
	100	13,760	31,865	54,316	81,112

We study the cases for which  $13\,000 < S_1/\beta\sqrt{\beta} < 120\,000$

For  $S_1/\beta\sqrt{\beta} < 13\,000$  the amplification is not significant enough to determine a representative site period  $T_s$ .

For  $S_1/\beta\sqrt{\beta} > 120\,000$ , we ignore the case corresponding to  $H/L = 1$ ,  $\beta = 0.2$ ,  $H_1/H = 1$  and  $S_1/\beta\sqrt{\beta} = 156\,000$  for which the site period goes back to low periods.

We observe a linear evolution of  $T_s$  with  $S_1/\beta\sqrt{\beta}$  (figure 17).

#### 4.3.3 Spectral ratio

As for 1D soil layers, we observe that, for a given period, spectra have a higher amplitude for soft soils (low  $\beta$ ) (figure 18).

By analogy with the 1D case we propose a representation of  $(SR - 1) \cdot S_1$  as a function of the parameter  $S_1/\beta\sqrt{\beta}$

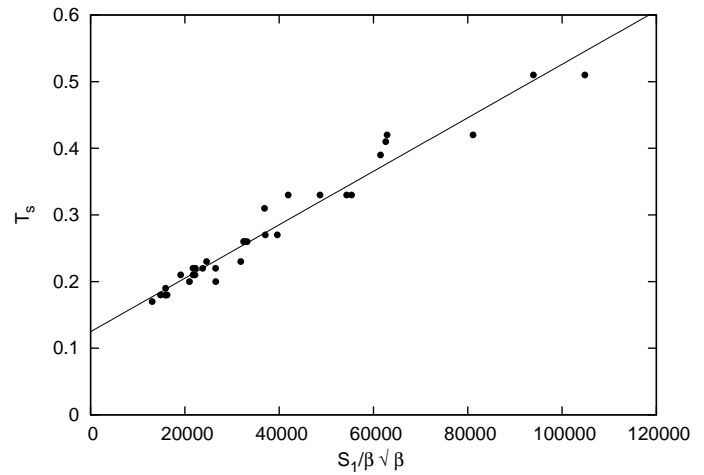


Figure 17. Evolution of the site period with  $S_1/\beta\sqrt{\beta}$  for trapezoidal valleys

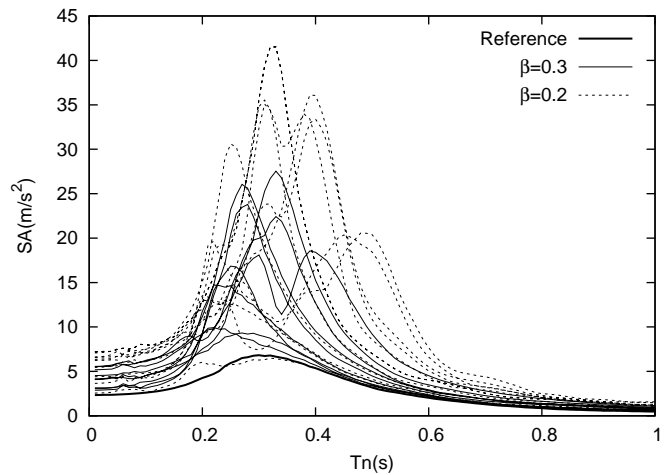


Figure 18. Response spectra for trapezoidal valleys

governing the site period. The numerical results we obtained for trapezoidal valleys are represented on figure 19. We eliminated one case ( $H/L = 1$ ,  $\beta = 0.2$ ,  $H_1/H = 1$ ,  $S_1/\beta\sqrt{\beta} = 156\,000$ ) for which the site period goes back to low periods.

The amplification is negligible up to a threshold corresponding to  $S_1/\beta\sqrt{\beta} = 13\,000$ . Afterwards, the evolution of  $(SR - 1) \cdot S_1$  with  $S_1/\beta\sqrt{\beta}$  shows a parabolic tendency.

From these curves, knowing the geometrical characteristics of the valley  $S_1$  and its soil properties  $\beta$ , we can now calculate the coefficient  $S_1/\beta\sqrt{\beta}$ . With this coefficient we can read an estimate of the site period  $T_s$  and the coefficient  $(SR - 1) \cdot S_1$  and then deduce the value of the spectral ratio  $SR$  (figure 17 and 19).

## 5 CONCLUSIONS

Although 2D complex site effects are not yet taken into consideration in building codes, many studies have pointed out the importance of their impact on seismic movement. Indeed, these site effects often lead to a higher amplification of the seismic signal compared to the 1D case. It also causes an extension of the signal length.

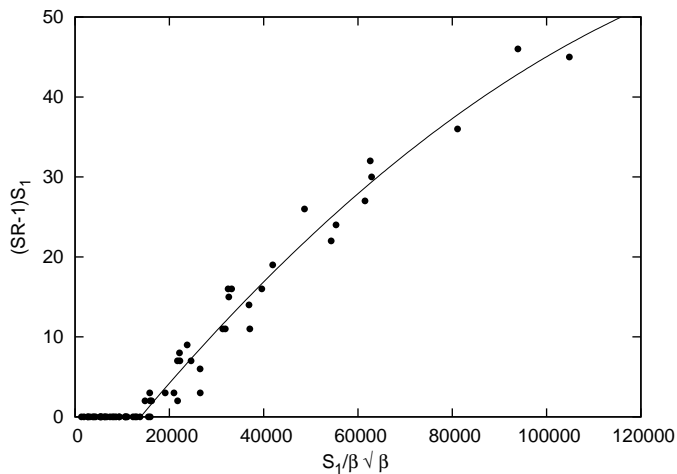


Figure 19. Evolution of  $(SR - 1) \cdot S_1$  with  $S_1/\beta\sqrt{\beta}$

This study gives a method to characterise the spectral amplification of bidimensional trapezoidal valleys with various geometrical characteristics and soil properties. Two parameters, the site period and the spectral ratio, were used to characterise spectral amplification. We considered valleys with shape ratios  $H/L$  lower than 1 and impedance contrast higher than 0.2.

We first found again known results :

- For 1D soil layers we found a good correlation with the analytical solution. Indeed, the maximum amplification of the acceleration response spectrum occurs for the natural period corresponding to the fundamental frequency of the soil layer.
- For empty valleys, the maximum amplification occurs at the edge of the valley.
- In fully-filled valleys, the maximum amplification takes place at the centre of the valley.
- When increasing the filling ratio, we go from empty valley behaviour to fully-filled valley behaviour.

The main results of this study are :

- At the central point of the valley, the evolution of the site period  $T_s$  with the parameter  $S_1/\beta\sqrt{\beta}$  has a linear tendency. This parameter combines the soil properties and the geometrical characteristics of the valley.
- At the centre of the valley we can estimate the spectral ratio  $SR$  from the curve representing the evolution of  $(SR - 1) \cdot S_1$  as a function of  $S_1/\beta\sqrt{\beta}$  (figure 19).

As a conclusion, the approach consisting in characterising spectral amplification by the site period and the spectral ratio has lead to interesting results. Indeed, a simple criterion, combining geometrical characteristics and soil properties, has been proposed. This criterion allows for estimates of the site period and the spectral ratio. But the cases we studied were limited and took into account only a few parameters. This study could therefore be extended to other shapes, softer soils or different input wave characteristics. Validating these results with experimental data would also be useful.

REFERENCES

[1] M.D. Trifunac, "Surface motion of a semi-cylindrical alluvial valley for incident plane SH waves," *Bulletin of the Seismological Society of America*, vol. 61, no. 6, pp. 1755-1770, 1971.

[2] M.D. Trifunac, "Scattering of plane SH waves by a semi-cylindrical canyon," *Earthquake Engineering & Structural Dynamics*, vol. 1, no. 3, pp. 267-281, 1972.

[3] H.L. Wong and M.D. Trifunac, "Scattering of plane SH waves by a semi-elliptical canyon," *Earthquake Engineering and Structural Dynamics*, vol. 3, no. 2, pp. 157-169, 1974.

[4] H.L. Wong and M.D. Trifunac, "Surface motion of a semi-elliptical alluvial valley for incident plane SH waves," *Bulletin of the Seismological Society of America*, vol. 64, no. 5, pp. 1389-1408, 1974.

[5] F.J. Sanchez-Sesma, "Diffraction of elastic SH waves by wedges," *Bulletin of the Seismological Society of America*, vol. 75, no. 5, pp. 1435-1446, 1985.

[6] Y. Nakamura, "A method for dynamic characteristics estimation of subsurface using microtremor on the ground surface," *Railway Technical Research Institute, Quarterly Reports*, vol. 30, pp. 25-33, 1989.

[7] B. Gatmiri and M. Kamalian, "Two-dimensional transient wave propagation in anelastic saturated porous media by a Hybrid FE/BE method," in *Proceedings of the fifth European Conference on Numerical Methods in Geotechnical Engineering*, 2002, pp. 947-956.

[8] B. Gatmiri and K. Dehghan, "Applying a new fast numerical method to elasto-dynamic transient kernels in HYBRID wave propagation analysis," in *Proceedings of sixth conference on structural dynamics (EURODYN 2005), Paris, France. Rotterdam : Millpress*, 2005, pp. 1879-1884.

[9] B. Gatmiri and C. Arson, "Seismic site effects by an optimized 2D BE/FE method II. Quantification of site effects in two-dimensional sedimentary valleys," *Soil Dynamics and Earthquake Engineering*, vol. 28, no. 8, pp. 646-661, 2008.

[10] B. Gatmiri, P. Maghoul, and C. Arson, "Site-specific spectral response of seismic movement due to geometrical and geotechnical characteristics of sites," *Soil Dynamics and Earthquake Engineering*, vol. 29, no. 1, pp. 51-70, 2009.

[11] S.L. Kramer, *Geotechnical earthquake engineering*, Prentice Hall, 1996.